Annales Geophysicae, 23, 1821–1838, 2005
SRef-ID: 1432-0576/ag/2005-23-1821

Annales Geophysicae

Combined optical, EISCAT and magnetic observations of the omega bands/Ps6 pulsations and an auroral torch in the late morning hours: a case study

V. Safargaleev [1,2], T. Sergienko [2], H. Nilsson[2], A. Kozlovsky[3,4], S. Massetti[5], S. Osipenko[1], and A. Kotikov[6]

[1]Polar Geophysical Institute, Apatity, 184200, Russia
[2]Swedish Institute of Space Physics, S-981 28, Kiruna, Sweden
[3]Department of Physical Science, University of Oulu, Oulu, FIN-90014, Finland
[4]Sodankylä Geophysical Observatory, Sodankylä, FIN-99600, Finland
[5]Instituto di Fisica dello Spazio Interplanetario, 00133, Rome, Italy
[6]Institute of Physics, St.Petersburg State University, St. Petersburg, 198504, Russia

Received: 15 September 2004 – Revised: 24 March 2005 – Accepted: 5 April 2005 – Published: 28 July 2005

Abstract. We present here the results of multi-instrument observations of auroral torch and Ps6 magnetic pulsations, which are assumed to be the magnetic signature of the spatially periodic optical auroras known as omega bands. Data from TV and ASC cameras in Barentsburg and Ny Ålesund, EISCAT radars in Longyearbyen and Tromsø, as well as IMAGE network were used in this study. The auroral phenomenon which was considered differed from that previously discussed, as it occurred both in an unusual place (high latitudes) and at an unusual time (late morning hours). We show that this might occur due to specific conditions in the interplanetary medium, causing the appropriate deformation of the magnetosphere. In such a case, the IMF turned out to be an additional factor in driving the regime of Ps6/omega bands, namely, only by acting together could a substorm onset in the night sector and B_z variations result in their generation. Since the presumable source of Ps6/omega bands does not co-locate with convection reversal boundaries, we suggest the interpretation of the phenomena in the frame of the interchange instability instead of the Kelvin-Helmholtz instability that is widely discussed in the literature in connection with omega auroras. Some numerical characteristics of the auroral torch were obtained. We also emphasize to the dark hole in the background luminosity and the short-lived azimuthally-restricted auroral arc, since their appearance could initiate the auroral torch development.

Keywords. Magnetospheric physics (Auroral phenomena; Plasma convection; Solar wind-magnetosphere interaction)

Correspondence to: V. Safargaleev
(safargaleev@pgi.kolasc.net.ru)

1 Introduction

Among others, one remarkable auroral form allowing the investigation of magnetospheric phenomena via the visible features is the large-scale (up to 1000 km in azimuthal direction) luminosity undulations of the poleward boundary of diffuse auroras first described by Akasofu and Kimball (1964) and named "omega bands" due to their similarity with an inverted (open to the pole) Greek letter Ω. In contrast to auroral arcs, which are indeed the predominant form of auroras, the omega bands are rather rare observational phenomena, probably due to the small extension in the NS direction that creates a difficulty for a ground observer to distinguish them on the all-sky images from a dished auroral arc. For this reason relatively little attention has been paid to omega bands and only a limited number of publications devoted to this kind of auroral activity can be found. So the main morphological features of the Ω-bands do not seem to be well established, nor has a complete understanding of their nature been achieved. To prove this, we review briefly the main results of the past studies, emphasizing the differences introduced by the more recent investigations.

Using the DMSP-2 photographs, Akasofu (1974) found that the poleward boundary of diffuse auroras tends to develop a well-defined wavy structure (i.e. omega bands) most often in the morning sector and sometimes in the midnight sector. Recently, several cases of similar optical phenomena have also been reported in the evening sector (Solovyev et al., 1999).

The Ω-band formation was connected traditionally with the preceding substorm activity (Akasofu, 1974), namely the substorm recovery phase (Opgenoorth et al., 1994). However several cases have been presented showing that these auroras seem to be a typical feature of steady magnetospheric

convection events (see Solovyev et al., 1999 and references therein).

A sequence of localized field-aligned currents with alternating directions can be associated with the omega bands. These currents in combination with ionospheric currents form a stationary (in time) current system that travels in the azimuthal direction, creating magnetic pulsations on the ground (Kawasaki and Rostoker, 1979) which were reported earlier by Saito (1978) as a subclass of Pi3 pulsations. These pulsations, nominated as Ps6, occurred predominantly in the declination among the three components and had periods of 5–40 min. Saito pointed out the possible connection between the Ps6 and some kinds of spatially periodic auroral forms: substorm surges, auroral arc loops and Ω-bands observed in the same local time sector as the Ps6. However, he could not present a simultaneous observation of both (optical and magnetic) phenomena. Later, on the basis of results obtained with simultaneous multi-instrument observations, André and Baumjohann (1982), Opgenoorth et al. (1983), and Steen et al. (1988) showed that the Ω-bands and the positive spikes in the D- or Y-component (Ps6 pulsations) may be regarded as the same phenomenon seen by different instruments. This led some investigators to identify Ω-bands by means of ground-based magnetometer data, even when optical images were not available (Lühr and Schlegel, 1994; Jorgensen et al., 1999; Wild et al., 2000) or have too a low spatial resolution as a result of being taken from high altitudes (Connors and Rostoker, 1993). In accordance with early results, one of the morphological features of the Ps6 is their association with magnetospheric substorms (Saito, 1978). Connors et al. (2003) recently claimed that Ps6 disturbances should not be viewed primarily as phenomena related to the substorm recovery phase. In general, this finding hinders the use of the Ps6 as a tool for omega band diagnostics, which are predominantly the recovery phase phenomena.

Signatures of omega bands have also been identified in the magnetosphere. Steen et al. (1988) discussed a modulation of the high-energy particle intensity at the geostationary orbit as a magnetosphere signature of omega bands. Using one of the Tsyganenko magnetic field models, Tagirov (1993) has shown that the auroral torches are magnetically linked to the equatorial plane of the magnetosphere to a distance of 5–6 R_E, which is consistent with the result derived by Steen et al. (1988). Jorgensen et al. (1999) also concluded that omega bands are the electrodynamic signature of a corrugated inner edge of a current sheet in the near-Earth (geostationary) magnetosphere. A different location of the Ω-band and source in the magnetosphere was reported by Pulkkinen et al. (1991). Using the Tsyganenko model, they showed that the omega bands and Ps6 events are mapped to the current sheet region between 6 and 13 R_E.

Akasofu (1974) suggested that in very active situations the bright auroral tongues separating the dark holes of the omega bands can develop into torch-like structures extending toward the pole. According to DMSP photographs, the size of a torch can vary from a few hundred to several thousand kilometers. Both the omega bands and torches are usually observed to drift eastward at a velocity of 0.4–2 km/s (Opgenoorth et al., 1983; Steen et al., 1988), retaining their shape for several minutes. Oguti et al. (1981) showed that torches may have a spatial structure consisting of a nonpulsating periphery and a pulsating core. By comparing simultaneous photographs of auroras from two stations, Opgenhoorth et al. (1983) has found the altitude of the torch to be 100 km. In accordance with Tagirov (1993), the altitude of the poleward boundary of nonpulsating periphery of the torch is less than 100 km, which indicates that it is formed by particles with a characteristic energy of more than 10 keV.

For lack of observational results, at present there is no commonly accepted understanding of the formation mechanism of omega bands, as well as the torch-like structures. At least three kinds of plasma instabilities are discussed as a candidate magnetospheric generator of the spatial luminosity undulations in the ionosphere. Rostoker and Samson (1984) suggested that the Kelvin-Helmholtz instability (KHI) leads to generation of omega bands. The instability should develop at the boundary between the boundary layer plasma sheet and the central plasma sheet where a flow shear took place. Yamamoto et al. (1997 and references therein) connected the Ω-band and the torch formation with an instability quite similar to the Rayleigh-Taylor ("interchange") instability developing on the outer boundary of hot plasma torus. This boundary was assumed to appear during the substorm recovery phase. The instability of the magnetosphere-ionosphere system, which also resulted in the omega-like structures, was discussed theoretically by Lyatsky and Maltsev (1984) (see also Tagirov, 1993), while numerical modeling was performed by Janhunen and Huuskonen (1993). Also worth mentioning is a mechanism described by Jorgensen et al. (1999), who assumed that the waves excited on the inner edge of the current sheet are responsible for optical omega-band generation via the production of the field-aligned electric fields causing spatially-periodic electron precipitations.

In this paper we discuss a case of coordinated EISCAT and TV observations of an auroral torch formation. Since the torch was observed in the late morning sector (∼09:00 MLT) and at high latitudes (∼75° corrected geomagnetic latitude, CGMLAT), which is non-typical for such auroras, one of the aims of this paper was to extend the statistics on the morphology and dynamics of omega auroras. Unfortunately, the bad weather conditions southward of the observational point prevented a detailed study of the omega band from which the torch originated, and we had to limit ourselves to a detailed analysis of the torch itself, namely by combining the optical and radar measurements, we tried to understand the reasons which cause the poleward stretching of one of the bright Ω-band and tongues.

2 Instrumentation

The considered "torch event" took place during the Swedish-Finnish EISCAT experiment carried out by the Swedish Institute of Space Physics (IRF, Sweden) and the University of

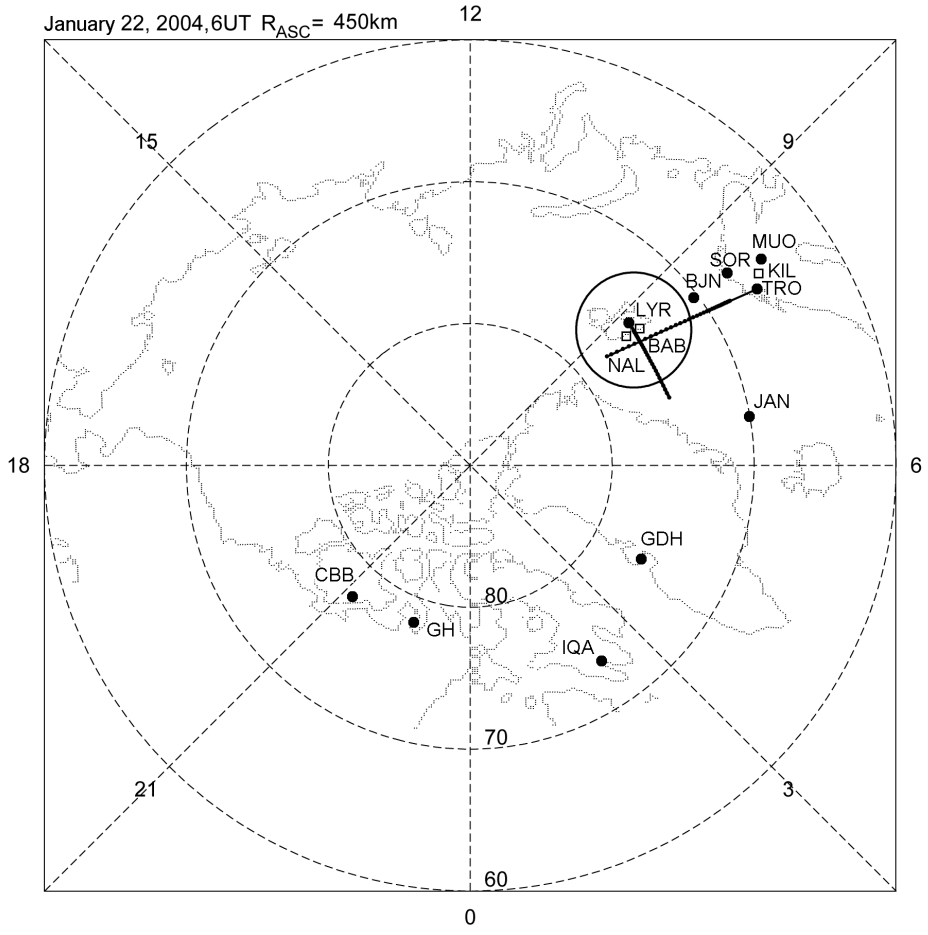

Fig. 1. Location of observational points. Black circles indicate magnetic observatories, open squares show the location of optical instruments, large circle is the BAB TV camera field of view, the EISCAT Svalbard and the EISCAT UHF beams are shown with bold lines.

Oulu (Finland), in cooperation with the Polar Geophysical Institute (PGI, Russia) on 19–27 January 2004 in the Spitsbergen archipelago. The aim of the campaign was to investigate the dynamics of dayside auroras through coordinated radar and optical measurements.

The ionospheric plasma flow was monitored by the EISCAT Svalbard radar (the ESR) located near Longyearbyen (LYR) and the mainland EISCAT UHF radar located close to the city of Tromsø (TRO). The ESR radar system consists of two antennas; the 32-m steerable dish which can be pointed in any direction and the 42-m dish which is fixed along the magnetic field-line direction. The ESR-32-m antenna was pointed west at a 45° elevation, which allowed us to measure the ionospheric plasma flow along the east-west direction in the F-region (above 200 km). The mainland UHF radar was pointed the north at a low elevation (20°), which allowed for observations of the north-south ionospheric plasma flow along the geomagnetic meridian. At the latitude of the Svalbard site, the UHF radar was measuring at heights of the order of 400 km. The key optical instrument of this study was the TV camera from the Polar Geophysical Institute (Russia) installed ∼40 km west of the Svalbard radar site, at the village of Barentsburg (BAB). This camera provided high-resolution optical measurements of auroras in white light. The field of view of this camera is shown in Fig. 1 by a circle while the two solid lines indicate the Svalbard and Tromsø radar beams.

For monitoring the auroral activity both poleward and equatorward of Barentsburg, the data of the ASC cameras of the Finnish Meteorological Institute (Finland) running at Kilpisjarvi (KIL) and of the Istituto di Fisica dello Spazio Interplanetario (Italy) running at Ny Ålesund (NAL) were also used. Several appropriately located magnetic observatories of the International Real-time Magnetic Observatory Network (INTERMAGNET) and the Magnetometer Array for Cusp and Cleft Studies (MACCS) supplied the information about substorm activity in the night sector (west–east chain). The meridional distribution of Ps6 pulsations was inferred from the northern part of the IMAGE network (north–south chain). The standard set of IMAGE stations (NUR–NAL chain) was used to reconstruct the meridional distribution of ionospheric equivalent currents. Geographic and geomagnetic coordinates of the observatories, as well as MLT midnight, are presented in Table 1. In Fig. 1 the magnetic

Table 1. List of observatories.

Code	Name	Geographic		Corrected geomagnetic		loc.midnigh, UT
		lat (°)	long (°)	lat (°)	long (°)	
West-East chain						
CBB	Cambridge Bay	69.10 N	105.0 W	77.05	309.92	07:52
GH	Coral Harbour	64.1 N	83.2 W	73.90	350.29	05:38
IQA	Iqaluit	63.75 N	68.52 W	72.49	14.55	04:08
GDH	Godhavn	69.25 N	53.53 W	75.50	38.98	02:28
JAN	Jan Mayen	70.90 N	8.70 W	70.29	82.93	22:55
North-South chain						
NAL	Ny Ålesund	78.92 N	11.93 E	76.26	110.98	20:55
LYR	Longyarbyen	78.20 N	15.83 E	75.31	111.88	20:51
BAB	Barentsburg	78.05 N	14.12 E	75.29	110.46	20:56
BJN	Bjornøya	74.50 N	19.00 E	71.52	107.76	21:05
SOR	Sørøya	70.54 N	22.22 E	67.40	106.08	21:11
TRO	Tromsø	69.66 N	18.94 E	66.69	102.79	21:24
MUO	Muonio	68.02 N	23.53 E	64.43	105.90	21:14

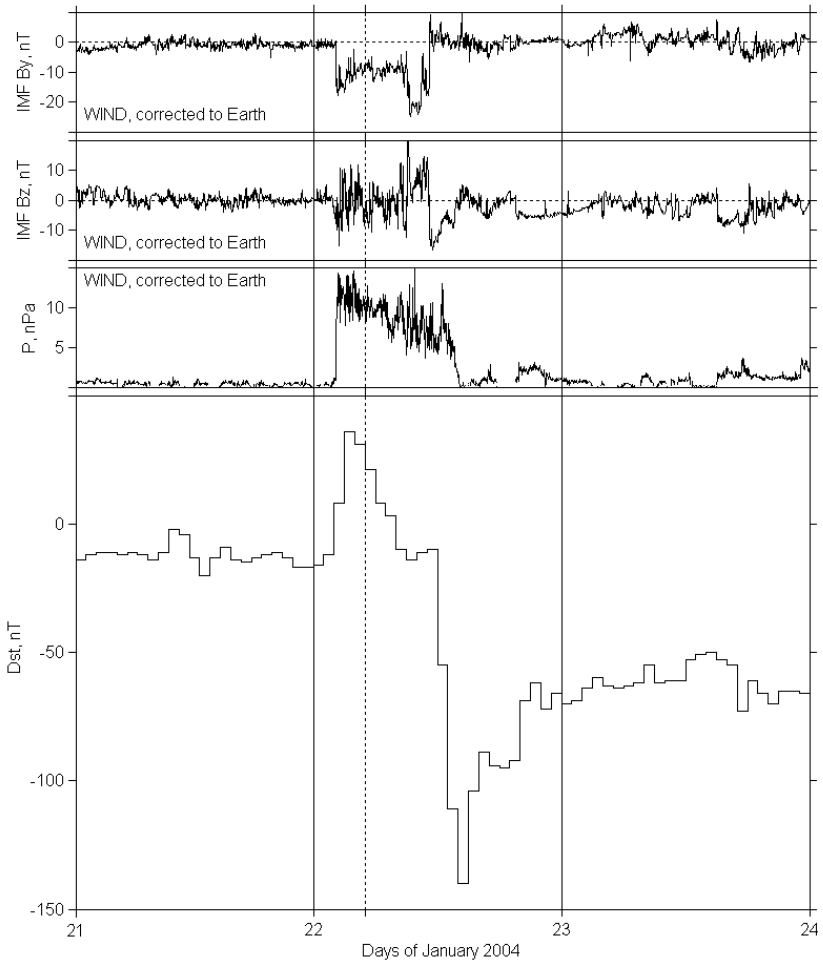

Fig. 2. The signatures of the magnetic cloud in space (three top plots) and on the ground. The time of torch observation is indicated with a vertical dashed line at 06:03 UT.

stations of both W–E and N–S chains are shown with black circles, while open squares indicate the position of the optical instruments. The data on the interplanetary medium were taken from the WIND satellite.

3 Development of omega auroras and an auroral torch on 22 January 2004

3.1 Geomagnetic background

On 22 January 2004 a magnetic cloud passed by the Earth and initiated a magnetic storm of about 150-nT intensity as measured by the D_{st} index (Fig. 2). The leading front of the cloud reached the Earth at ∼01:37 UT, indicated by a step-like increase of the magnetic horizontal component at the low-latitude station Kakioka (sudden impulse, SI). Thirty minutes later a sudden increase in the solar wind dynamic pressure of about ∼10 nPa was detected by the WIND satellite probing the solar wind at the evening flank of the distant magnetotail (x=–210 R_E, y=42 R_E, z=4 R_E). This time delay is ∼8 min less than the expected propagation time of the solar wind irregularity estimated as $\Delta t = x / V_{SW}$, where V_{SW}=630 km/s is the x-component of solar wind velocity and x is the distance between the satellite and the subsolar point on the magnetopause. Therefore, the WIND data presented in the paper have been shifted by 35 min in time.

The magnetosphere compression was accompanied by a positive D_{st} variation and a large value of the planetary K_p index (K_p=5). The torch was observed four hours after the D_{st} enhancement and six hours before the D_{st} negative bay (magnetic storm). In Fig. 2 this time is indicated with a vertical dashed line. This would imply that neither the SI nor the magnetic storm onset might be regarded as an immediate "trigger" of the auroral torch.

As might be inferred from INTERMAGNET and MACCS magnetic data, at least two substorms took place in the night sector in response to the magnetic cloud pass. The onset closest to the moment of interest started near 05:00 UT. The variations in the magnetic H-component at observatories located approximately along the CGMLAT of the BAB are shown in Fig. 3a, with the most westward one at the top. The onset signature (negative H-bay) has its largest magnitude at GH and GDH stations located poleward of IQA and JAN. This fact, as well as the time delay between the bay onset at the GH and LYR with respect to GDH, indicates that the substorm current wedge developed from the distant magnetotail in the post-midnight-early morning sector. One more negative bay was also seen at lower latitudes (IQA and JAN) ten minutes before the onset, which on the high latitude stations (GDH and GH) looked like the signature of a substorm preliminary phase. The onset near 05:00 UT was accompanied by the Ps6 disturbances in the late morning sector, as observed by the IMAGE network. Figure 3b emphasizes this by plotting the perturbations in the Y-component from the TRO observatory. The torch was observed at the end of the recovery phase (vertical solid line in Fig. 3a).

As we are dealing with the dayside phenomenon, generally well correlated to the incoming solar wind conditions, it would also be reasonable to try to associate the auroral torch with the interplanetary parameters. Trondsen et al. (1999) reported that strong undulations in the poleward boundary of the dayside part of the auroral oval may take place if the IMF B_y component is largely positive. However, the IMF B_y component was large and negative during our event. There were several northward turnings of the IMF B_z component during a 30-min interval preceding the torch observation. The possible role of those variations on the omega bands generation will be discussed in Sects. 3.3.1 and 4.2.

3.2 Optical observations

On 22 January 2004 the TV observation at BAB started at 05:30 UT. So, for monitoring of the auroral activity we used data from a digital all-sky camera (NAL) running ∼100 km north of Svalbard EISCAT site. The aurora dynamics for the 1.5-h interval preceding the torch formation are presented in Fig. 4 in the form of keograms and, in general, might be described as follows. Ten minutes before the substorm onset no significant auroras were seen in green emission. A few minutes after onset two kinds of green auroras appeared in the ASC field of view. The first was characterised by bright multiple arcs near zenith. These arcs might be identified with "Sun-aligned" arcs (Shiokawa et al., 1997), which are assumed to be the azimuthal extension to the dawn of the substorm nightside auroras (Safargaleev et al., 2003). The second was the wide band of rather faint multiple diffuse arcs (as was inferred later from the BAB TV data), the appearance of which on the southern horizon near 05:03 UT coincided with the beginning of a negative H-bay at GDH. At 05:55 UT the intensity of the auroras started to increase in the southern half of the BAB TV camera's field of view, except for a small area south-west of the BAB zenith, and the wave-like structures (the Ω-bands) became discernible on the southern horizon at 06:01:50 UT. Approximately 2 min later the formation of the auroral torch began. In Fig. 5 we present a sequence of TV images showing the west-east propagation of the torch. The second (from the top) series illustrates the presence of a core of the torch whose intensity varies in time. The TV registration allowed for the estimation of a quasi-period of core pulsation as a few tens of seconds. Such spatial structure (pulsating core and non-pulsating periphery) is one of the characteristics of this kind of aurora (Oguti et al., 1981). After the torch passage the rayed multiple arcs appeared to be shifted poleward of the BAB zenith (bottom series of images). Below we describe the auroral activity around the torch formation in more detail, pointing out the more important features.

We suggest that the omega bands were developed between Bear Island (BJN) and the Scandinavia peninsula. In the BAB TV data, shown in Fig. 6a, the omega bands are seen as wave-like structures on the southern horizon. For better visualization of the structures, we emphasized their border with a thin white curve (image on the right). Although the clouds above northern Scandinavia hindered the observations of the

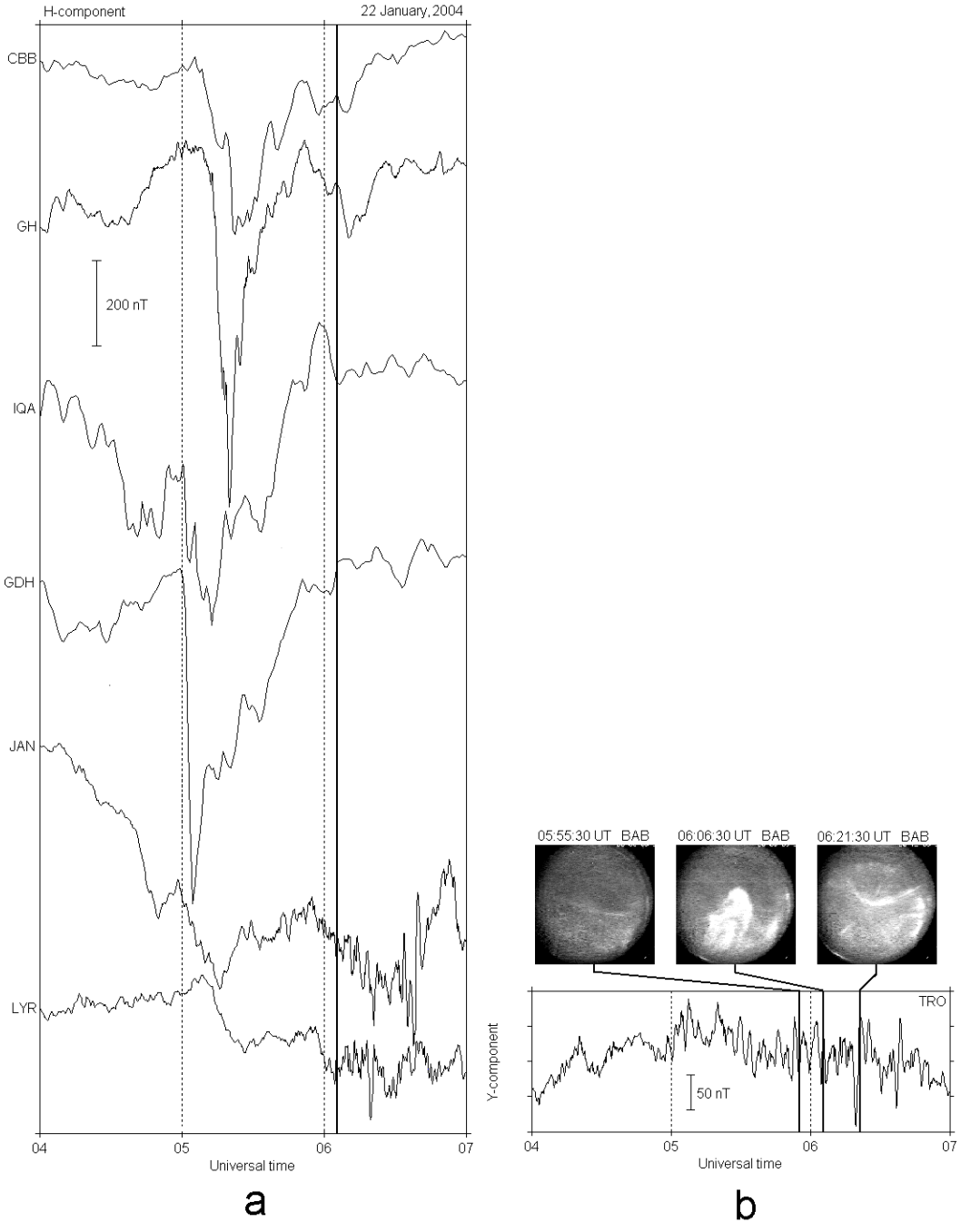

Fig. 3. (a) Substorm activity in the night side. Vertical bold line at 06:03 UT corresponds to the time of torch appearance. **(b)** Omega band-associated magnetic disturbances in the morning sector. The auroral torch (central image) and aurora activity before and after torch passage above BAB are also shown.

Ω-bands by the optical instruments located there, the magnetic signature of this kind of aurora (Ps6 pulsations) is seen at $\sim 67°$ CGMLAT in the data of the IMAGE magnetometer network. The series of images in Fig. 3b shows that Ps6 (and, hence, the omega bands) started one hour before the torch appearance and lasted much longer than the interval of torch observation. The latter assessment may also be confirmed by the photograph from the DMSP F13 satellite in Fig. 6b, taken at 07:00 UT.

The development of the torch began near 06:03 UT, as a poleward stretching of one of the bright tongues forming the omega bands (the most western undulation in the Fig. 6a). Beginning at 05:59 UT, one can distinguish a dark "hole" in the enhancing background luminosity, exactly at the place

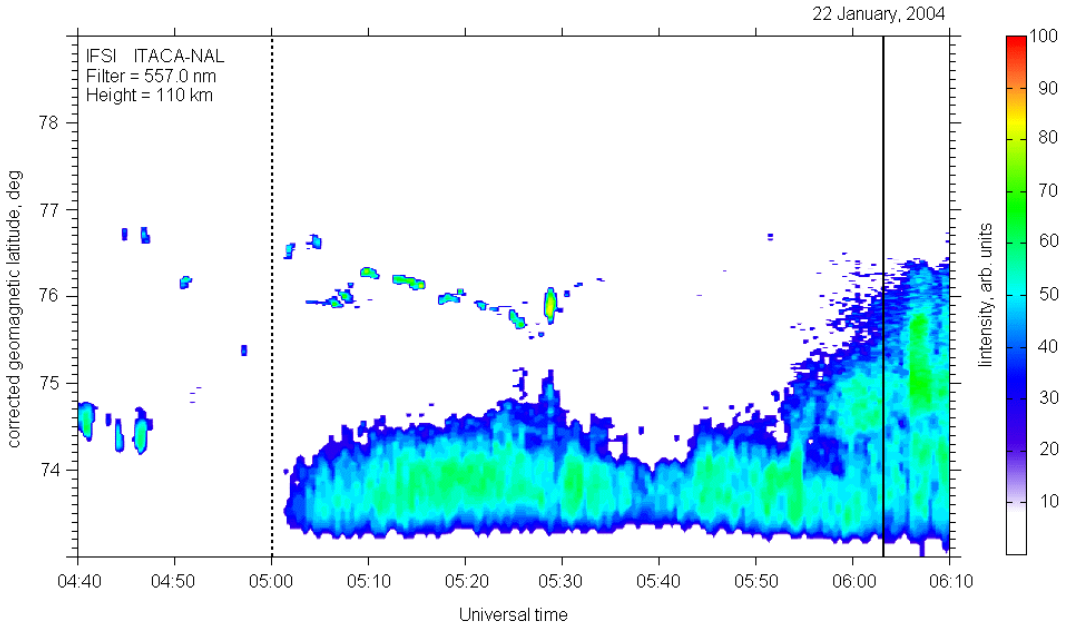

Fig. 4. Auroral activity above Spitsbergen as seen by ASC camera in Ny Ålesund. Dashed line indicate the substorm onset, bold line at 06:03 UT refers to the moment of torch appearance.

where the torch would appear a few minutes later. In the bottom image of Fig. 7a the border of the dark hole is emphasized with a thin black curve. Also shown are four squares: westward (red), eastward (green) and southward (blue) of the hole, as well as inside the hole (black square). The temporal variations of the sky luminosity averaged over these square areas are presented in Fig. 7b, showing that the aurora brightness inside the hole stopped increasing at ∼05:59 UT. We think that the dark area in the auroral background corresponded to the downward field-aligned current, whereas an upward current was associated with the faint arc seen in Fig. 7a, just poleward of the area occupied by brighter auroral forms.

At 06:02:30 UT the intensity of this arc started to increase. The use of two cameras separated by ∼40 km (BAB and LYR) allowed us to calculate the height of the arc. Before activation the arc was located at ∼160 km, whereas at the moment of maximum intensity the altitude of the arc dipped to ∼140 km. This indicated that the arc intensification was accompanied by electron acceleration. The height of the auroras corresponded to soft (∼300 eV) electrons coming, most probably, from the dayside extension of the boundary plasma sheet, BPS (Newell and Meng, 1992). The arc brightening was accompanied, as well, with its slight poleward displacement and with stretching, also poleward, of one of the Ω-bands tongues into the torch (upper series of images in Fig. 5). It is worth mentioning that one more torch-like form might be associated with the bright spot seen on the southeast edge of the TV frames. However, the north-south extension of this spot is rather small. This might be inferred from the comparison of two frames taken at 06:04:22 and 06:10:50 UT, seeing that in the latter the torch reached the same place on the sky as the spot on the former but its size in the NS direction is larger than the spot size. So we think that the spot was one of the undulations forming the omega auroras, rather than the torch, and that after 06:02:40 UT we observed, indeed, the formation of a single torch. At 06:06:20 UT (when the torch had been shaped) we calculated the height of its most poleward point to be in the range of 100–105 km, by means of triangulation between the BAB and NAL cameras. In this case, the height of the auroras corresponded to high-energy (∼5 keV) electron precipitation. This is consistent with either a central plasma sheet source (Newell and Meng, 1992) or a significant field-aligned acceleration of the colder plasma of boundary plasma sheet origin. No auroras were seen poleward of the torch while it moved through the camera's field of view. The above-listed features of auroral activity allow us to suggest that the auroral torch was associated with an azimuthally-restricted ionospheric plasma tongue which originated initially inside the CPS or BPS projection and expanded then poleward to the polar cap boundary. In the magnetosphere this plasma tongue may correspond to the flux tube moving outward from the Earth.

After the torch passage the rayed multiple arcs appeared on the sky (bottom series of images in Fig. 5). At approximately 06:14:35 UT one more auroral torch started to develop equatorward of these arcs. In the frame taken at 06:15:40 UT the main signature of the torch – a periphery and a core – may be distinguished. As in the situation discussed above, the small arc appeared poleward of the torch just before its formation (bottom left image in Fig. 5). But in contrast to the previous case, this torch was not so clearly manifested.

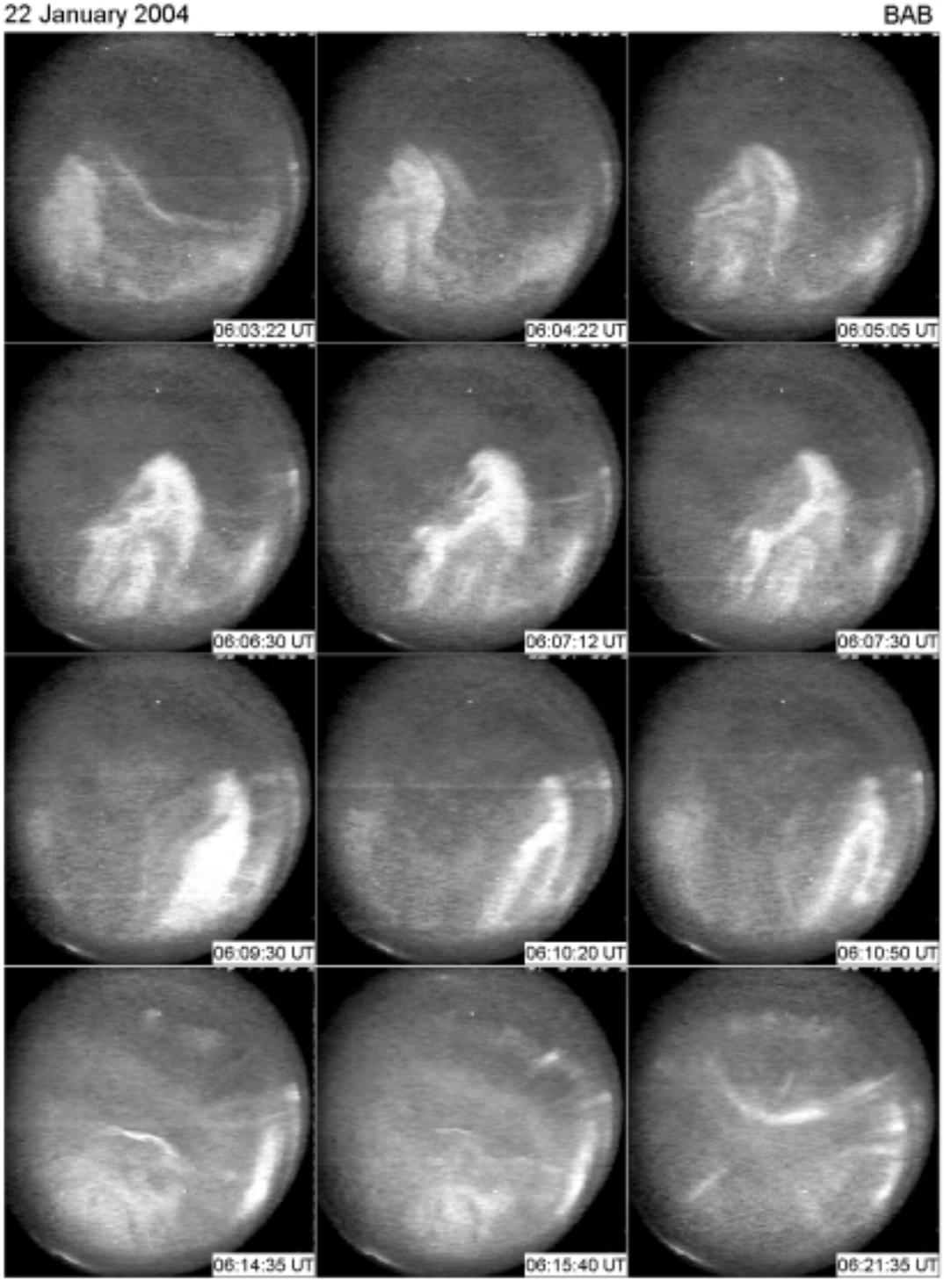

Fig. 5. Series of TV images showing the dynamics of auroras around the torch event. North (geomagnetic) is on the top, East is on the right.

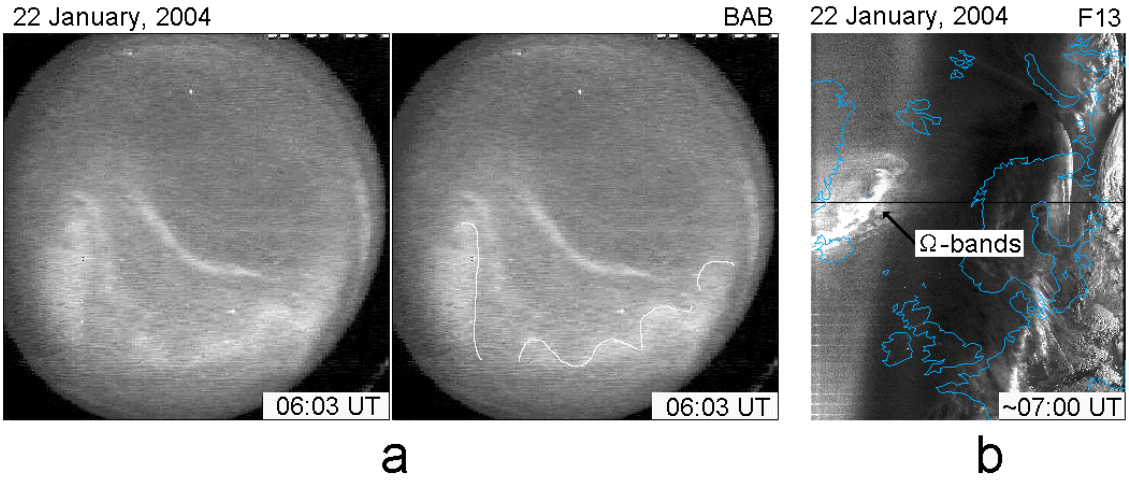

Fig. 6. Omega auroras before the torch passage as seen by the ground based TV camera **(a)** and after torch passage as seen from the DMSP satellite **(b)**.

3.3 EISCAT and IMAGE observations

3.3.1 The dynamics of the convection reversal boundary and auroral electrojet during Ps6 events as inferred from ESR-32-m and IMAGE network measurements

In general, the interval preceding the torch observation is characterized by poleward displacement of the convection reversal boundary in the vicinity of the observational points. This can be seen from a comparison of the ESR-32 data on the ion velocity (Fig. 8, upper panel) and the ionospheric currents calculated from the IMAGE data. The ESR radar in LYR measured the line-of-sight (l-o-s) convection velocity along the latitude (see Fig. 1). The algorithm of the ionospheric current reconstruction assumed that the currents flow predominantly along the geomagnetic latitude (Kotikov et al., 1991). In our case this is a valid assumption, since at 05:00 UT the IMAGE magnetometer chain is still located away from the place where the convection turns to the pole. Thus, as in the keogram, the contour map presented in Fig. 8 (bottom panel) in the "latitude-time" frame shows the dynamics of auroral electrojets along the meridian.

There are three intervals of positive (directed to the radar) l-o-s velocity in the radar data. The first one is between 04:40 and 05:00 UT, that is before the substorm onset, whereas two others – after 05:10 UT and before 05:40 UT – are related to the substorm recovery phase. Therefore, there is no reason to connect the appearance of the positive plasma flows (PPF) in the radar data with substorm activity directly, although the sign of velocity may mean that the ionospheric plasma entered from the nightside sector. As the flow of opposite direction followed the PPF, we suppose that the radar observed the N-S displacement of the convection reversal boundary which occurred in response to short-lived reductions of the polar cap, which were caused by the IMF B_z northward excursions (top plot in Fig. 8). The intensity of the PPF, as well as the PPF duration, increased from interval to interval and seems not to depend on the duration and amplitude of positive IMF B_z excursions. Such a feature of PPF may be explained by assuming that the convection boundary moved poleward approaching the radar beam from lower latitudes. The dynamics of the ionospheric Hall currents presented in Fig. 8 (bottom panel) support this assumption. Since the ions moved in the opposite direction to the Hall current, the zero line separating the eastward (blue contours) and westward (red contours) currents at the top of the map may be associated with the convection reversal boundary seen by the westward-directed antenna of the Svalbard radar at approximately the same CGMLAT. Some discrepancy is due to the poor coverage of the IMAGE observatories poleward of the Scandinavia coastline. Indeed, this boundary moved poleward and at the time corresponding to the intervals of PPF in radar data the westward electrojet underwent a momentary declination toward the radar beam, the position of which coincides on the map with the latitude of LYR.

The Ps6 disturbances started just after substorm onset at 05:00 UT and may also be associated with the formation of the equatorward boundary of the electrojet, as no pulsations were seen before that. The appearance of this boundary accompanied the pre-onset negative bays at IQA and JAN (or H-component enhancement at GDH and GH, which looked like the preliminary phase signature). Although this is important for understanding the reasons for omega band generation, the question of the electrojet formation refers more to the substorm morphology and its detailed analysis is beyond the scope of our study.

In Fig. 8 the Ps6 activity has the form of several trains. There is an apparent correlation between them and the N-S displacement of the electrojet and convection reversal boundaries. The maximum of the pulsation was observed during the southward shift of both the electrojet boundaries, whereas the beginning of Ps6 may be associated with maximum northward displacement of the electrojet equatorial

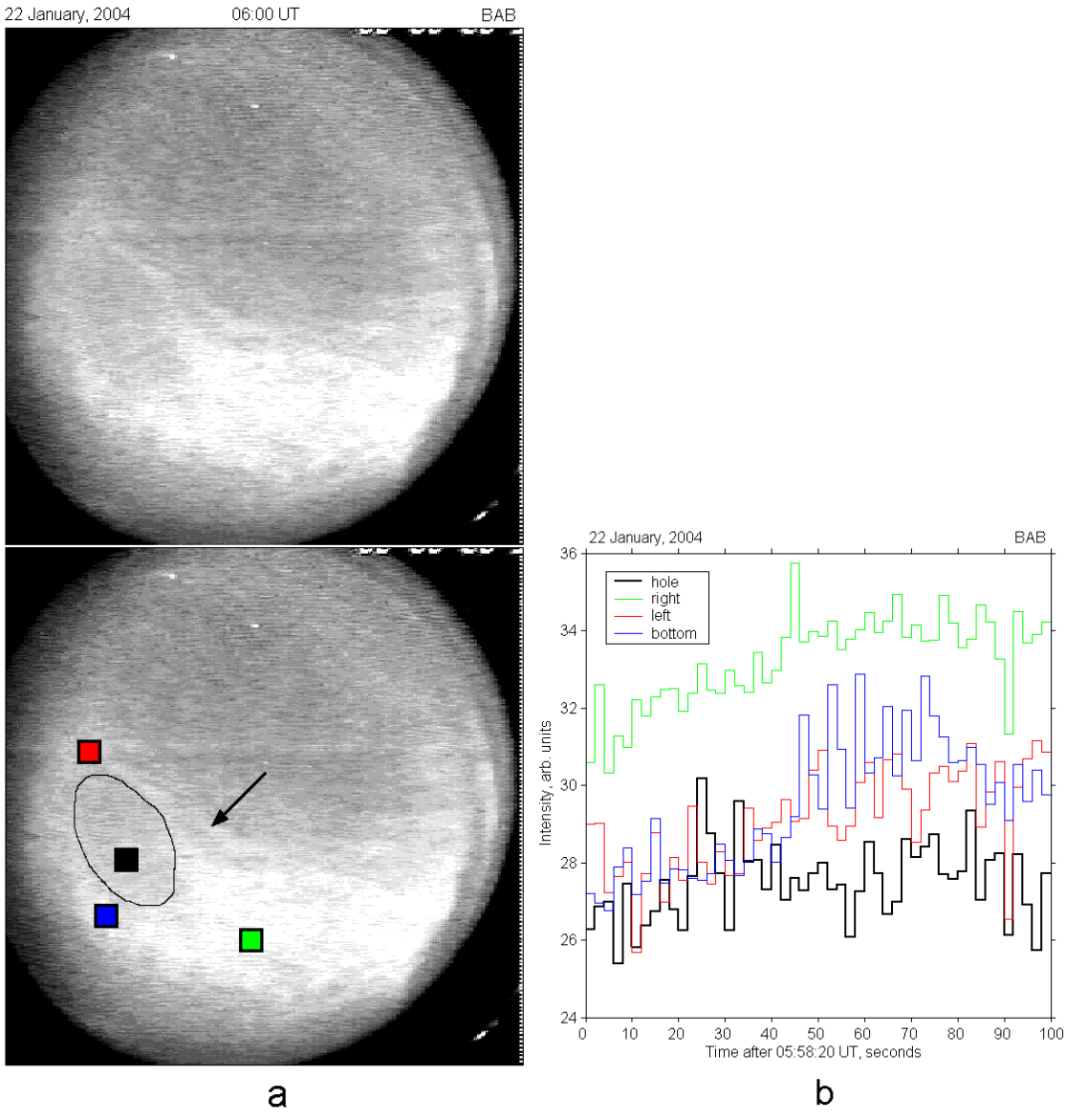

Fig. 7. The dark hole (outlined, in the lower image) in the enhancing diffuse auroras **(a)** and the sky luminosity variations in the square areas indicated in the lower image of the upper panel **(b)**. Black arrow indicates on the faint arc discussed in the text.

boundary that was closer to the SOR where the pulsations were the most manifested. Note that the Ps6 trains were also accompanied by electrojet intensifications (darker areas inside the electrojet on the contour map in Fig. 8). We regard these as one more manifestation of the omega auroras since the closing of the field-aligned currents associated with the omega bands in the ionosphere should enhance the ionospheric Hall currents (see Amm, 1996, for example).

3.3.2 The ULF and convection features accompanying the torch development

In this section we concentrate on BJN magnetic data since the amplitude of torch-associated disturbances was the largest for that station (Fig. 8, top panel). André and Baumjohann (1982) first presented coordinated optical and magnetic measurements during the passage of several wave-like auroral forms which they assumed to be the Ω-bands. In particular, they showed that this optical phenomenon was accompanied with positive variation in the east-west component of the geomagnetic field (see Fig. 3 in their paper). After that, the omega bands were commonly thought to be associated with a series of positive D-spikes (similar to that seen on the BJN magnetogram in Fig. 8 from 05:48 to 05:52 UT), even in absence of optical observations. In the case considered here, the torch was preceded by the D-component reduction at 05:59 UT which also looked like a spike and makes it unclear as to whether the torch passage was accompanied by positive or negative variations. This negative

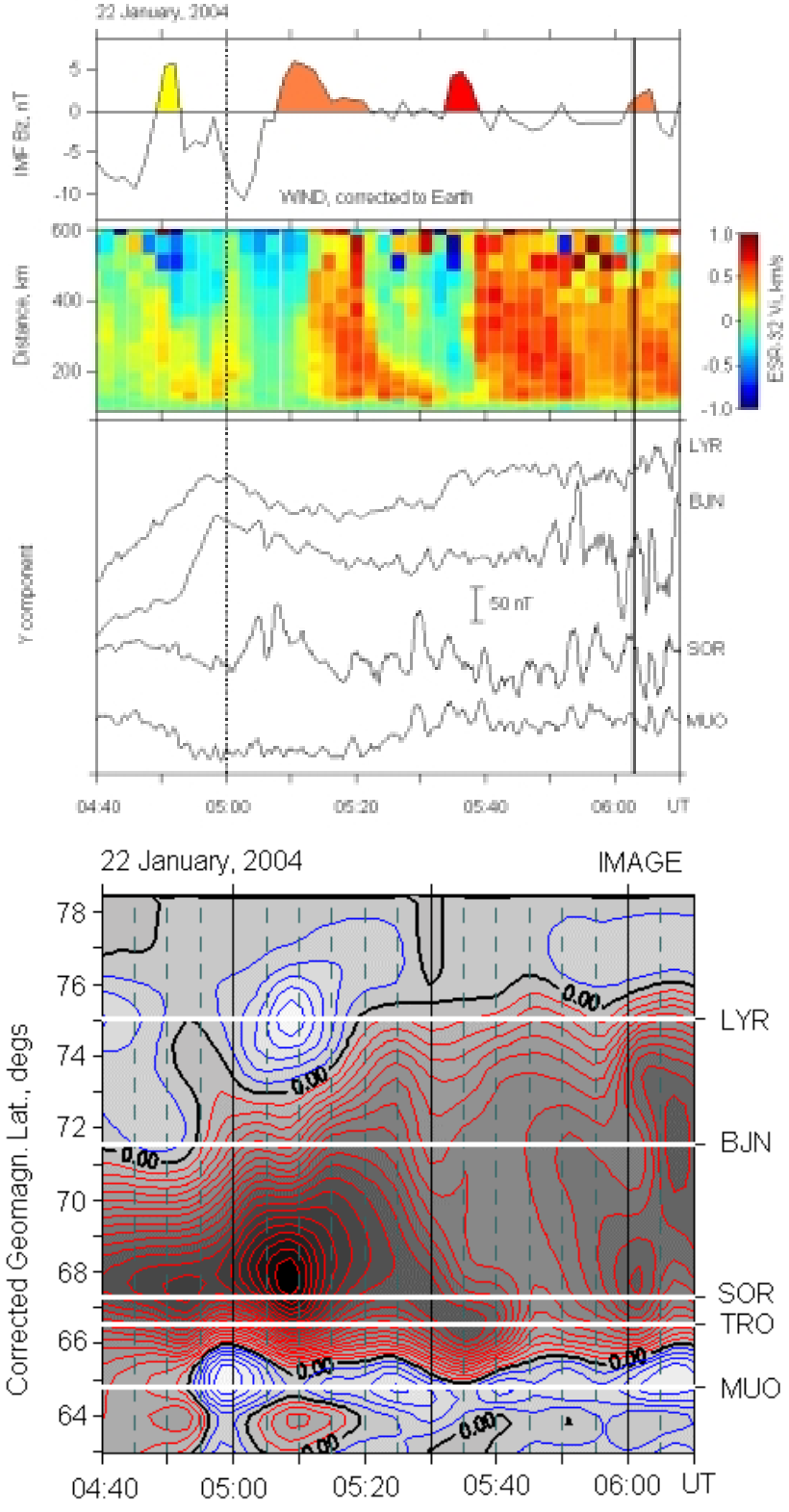

Fig. 8. Top panel: the azimuthal plasma flow and Ps6 activity are compared with the IMF B_z variations; the dashed line indicate the substorm onset, while the bold line refers to the moment of torch appearance, positive values of the velocity correspond to the plasma movement toward the radar. Bottom panel: dynamics of auroral electrojet; the red (blue) contours correspond to westward (eastward) Hall current, the darker areas indicate current enhancements.

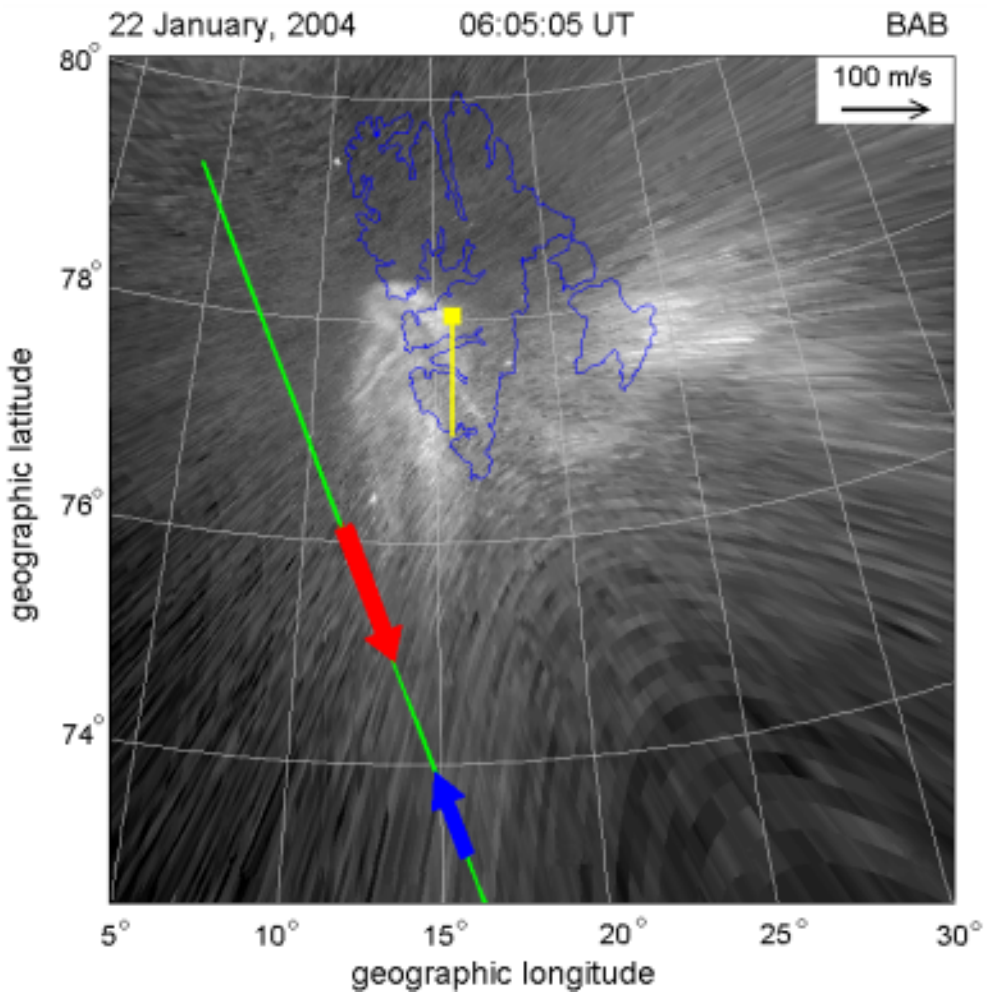

Fig. 9. Location of the EISCAT UHF beam (green line) and EISCAT Svalbard field aligned beam (yellow line) with respect to the auroral torch. The colored arrows are the line-of-sight velocities measured at 09:05 UT (see Fig. 10). The yellow square corresponds to the measurement point at altitude 115 km.

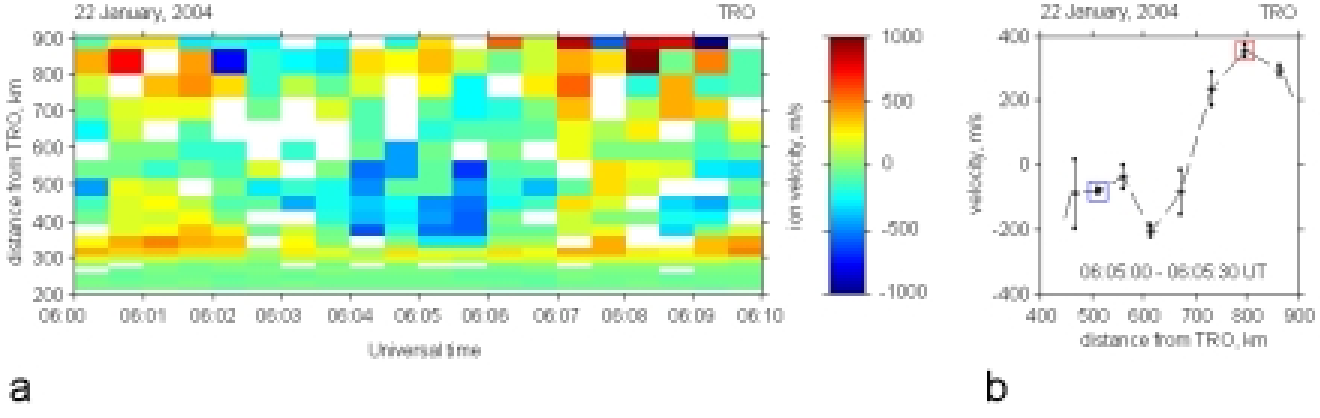

Fig. 10. **(a)** EISCAT UHF measurements of line-of-sight velocity in the vicinity of the westward torch border. Positive values correspond to a velocity toward the radar. **(b)** Distribution of l-o-s velocity along radar beam. The velocities plotted in Fig. 9 are here indicated with squares of the corresponding color.

spike-like variation coincided with the appearance of a dark hole in the background luminosity in Fig. 7b: a fact that is consistent with the findings of Opgenoorth et al. (1983), who showed the connection of northward equivalent ionospheric currents, causing the negative variation in the D-component, with downward field-aligned currents in dark areas of omega bands. A similar behavior – the increase a few minutes before the torch observation – demonstrated the D-component in the case on 21–22 October 1979 discussed by Opgenoorth et al. (1983) and Tagirov (1993) (Figs. 4 and 5, respectively). Consequently, we think that the enhancement of the downward FAC (manifested as the appearance of a dark hole in the background luminosity) may be considered as one of the precursors of torch development. We should note that this effect was not seen in the data presented by Steen et al. (1998). However, they dealt with the case of very intense Ps6 disturbances, which were at least five times larger than the ones discussed by Opgenoorth and in this paper. For this reason, this detail might be missed in their analysis.

Another observational result that provided useful insights into the mechanism of generation of the auroral torch was the feature of ionospheric convection near the torch border inferred from UHF radar measurements. The appropriate orientation of EISCAT antenna in Tromsø allowed the measurements of the ion's l-o-s velocity, which in our case was nearly the meridional (geomagnetic) component of the convection velocity, in several points inside the TV camera's field of view (see Fig. 1). Beginning at ∼06:03 UT, it measured the convection in the vicinity of the westward border of the developing torch. The location of the radar beam with respect to the torch is shown in Fig. 9, while the results of measurements are presented in Fig. 10. Since only the value of the velocity (inferred from the raw data with an error smaller than 30%) was taken into account, we removed the measurements done further than 900 km from Tromsø. The interval from 06:02 to 06:04 UT is characterized by numerous data gaps that occurred, probably, due to the high level of turbulence accompanying the torch development or low plasma density in the F region associated with the above-mentioned dark hole in the auroras. At 06:04 UT, the opposite plasma flows have formed in the vicinity of the westward border of the torch, namely at the points close to the radar site the ions moved northward, whereas at large distances the plasma flowed southward. This is well visible in Fig. 10b, where the distribution of the l-o-s velocity along the radar beam is shown for the temporal interval, when there were no data gaps in the radar data, and the torch border had been almost shaped. The plasma velocity at two measurement points located at distances 513 km and 864 km from the radar site is presented in Fig. 9 (blue and red arrows, respectively), together with the torch image projected on the ionosphere. The latest point lies outside the torch. The position of the former with respect to the torch is not so clear due to the clouds hiding the auroras at the south horizon and the projecting procedure also decreasing the aurora intensity toward the edge of image. However, if one produces in the mind's eye the torch's borders southward and takes into account the probable location of the omega auroras at the moment considered (see Sect. 3.2), it may be concluded that the blue arrow refers to the torch pedestal. In this place plasma moved poleward at a velocity 100±10 m/s, outside the torch plasma moved southward at a velocity 300±20 m/s. The point at 614 km seems to lie at the torch border (not shown in the figure). The drift velocity is also poleward here and has a larger value (200±20 m/s) than inside the torch.

4 Discussion

4.1 Brief summary on geomagnetic background

In this study we focus on an event that occurred on 22 January 2004 in the late morning hours (∼09:00 MLT) at high latitudes (L ∼16) during the pass of the Earth over the magnetic cloud. At that time K_p was 5, D_{st} was largely positive in response to a strong solar wind dynamic pressure (10 nPa), and IMF B_y was largely negative (–10 nT). Meng (1984) showed that during large negative D_{st} (i.e. during magnetic storms) both the cusp and poleward boundary of the nightside auroral oval are shifted equatorward, causing the polar cap expansion to lower latitudes. It is reasonable to assume that during large positive D_{st} an opposite effect – polar cap constriction and auroral oval shift poleward – should take place. In addition, the model simulations by Guzdar et al. (2001) also predict the reduction of the radius of the tail lobe cross section during periods characterized by high solar wind velocity, which is the condition existing in our case. Note also that high solar wind pressure should enhance the effectiveness of the interaction of the IMF with the magnetosphere (Newell and Meng, 1994), which could result in the fast and appreciable response of the polar cap dimension to B_z variations. A large negative B_y component would lead to the duskward displacement of the polar cap (Elphinstone et al., 1993) and to the twist of the magnetotail in the opposite direction. In the present case, the latter effect may be traced by the ground-based observations showing the maximum of substorm-associated H-bay at the GDH observatory, which was in the early morning sector (∼03:00 MLT) at that time. Probably due to all of these reasons, we were able to achieve an unusual observation of both the omega bands and an auroral torch, the source of which is usually attributed to the inner magnetosphere (L∼6–10) and which is typical of earlier MLT hours. Below we summarize the observations and discuss the possible generation mechanism for both the omega bands and the auroral torches.

4.2 Possible scenario for formation of omega auroras

The observations suggest that the Ω-bands were located somewhere between the Spitsbergen archipelago and the Scandinavian peninsula. Although these auroras were distinguishable on the DMSP F13 image, as well as on the frames of the TV camera running in Barentsburg, their detailed investigation was partially hindered by the poor weather conditions, and our conclusions are based mainly on analysis of

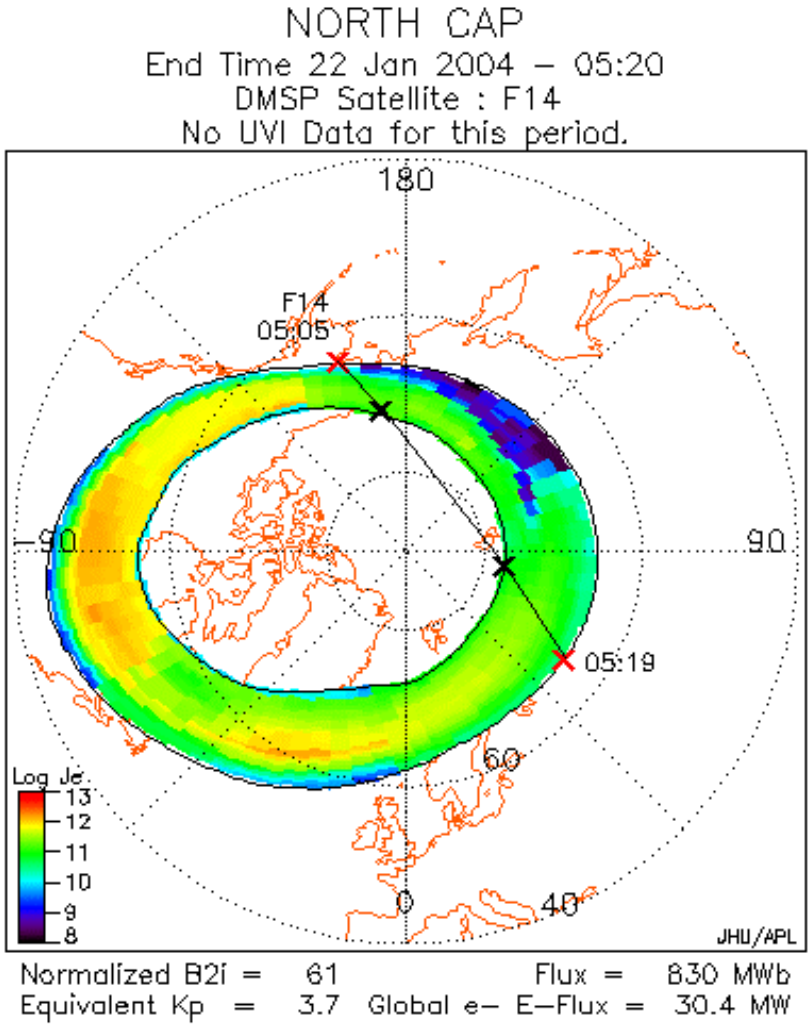

Fig. 11. Model of auroral oval at the beginning of Ps6 activity in local time–latitude (geographic) coordinates.

the disturbances in the geomagnetic Y-component (Ps6 magnetic pulsations) associated with the Ω-bands.

A substorm expansion phase onset at ∼05:00 UT on 22 January took place in the post-midnight-early morning sector. Simultaneously, large Ps6 disturbances started in the late morning sector, as observed by the IMAGE array stations in Scandinavia. The analysis of the data from these stations also indicates the appearance of the equatorial boundary of the westward electrojet between Tromsø and Muonio a few minutes before the substorm onset in the nightside. In Fig. 11 we present the location of the auroral oval calculated within the framework of the OVATION project (see description of the project at http://sd-www.jhuapl.edu/Aurora/ovation/index.html). Both poleward and equatorward borders of the oval coincide with the electrojet boundaries shown in Fig. 8 with an accuracy of ±1° CGLAT. One might connect the Ps6 with a Kelvin-Helmholtz instability which may develop at the electrojet borders associated with a shear flow. However, there are several details which argue against such an association, allowing for the interpretation of the phenomena within the framework of another kind of instability, the interchange instability, which has also been discussed in the literature in connection with omega auroras (Tagirov, 1993; Yamamoto et al., 1997; Sazykin et al., 2002). They are the following:

(1) No pulsations were measured at the LYR observatory, the observatory nearest to the convection reversal boundary in Fig.8, bottom, and the poleward edge of the auroral oval in Fig. 11, and this is not consistent with the idea of the omega bands being located near the boundary between BPS and CPS, as proposed by Rostoker and Samson (1984), or near the poleward boundary of the auroral oval, as proposed by Wild et al. (2000).

(2) Pulsations in the Ps6 range were more manifested near the equatorial boundary of the westward electrojet, but we have no direct (EISCAT) measurements proving the presence of opposite plasma flows there. From Fig. 8

we see that, close to 06:00 UT, the maximum of Ps6 shifted toward BJN, whereas the equatorward boundary of the westward electojet did not show any significant movement to the north. So the Ω-bands do not seem to be collocated with the opposite plasma flows near either the poleward or the equatorward boundaries of the auroral oval. Note that Connors et al. (2003) reported a case when the causative currents for Ps6 could be located inside the auroral oval and Lühr and Schlegel (1994) found that Ω-bands were embedded in a strong westward electrojet. Most probably, in our case the source of the Ps6/omega bands was inside the plasma sheet, away from its edges. The presence of auroras up to the latitude 74.5° during the Ps6 event also supports this conclusion (see keogram in Fig. 4).

(3) The Ps6 activity had a form of several trains coinciding in time with intervals of north-south movement of both the convection reversal boundary seen by the ESR at ∼75° CGMLAT and the westward auroral electrojet constructed from the IMAGE data. This means that the formation of convection reversal boundary alone did not result in the development of the instability responsible for the omega band generation (as should be in the case of K-H instability). There were some other factors which were manifested as the plasma sheet movement and did magnetospheric plasma unstable.

Although the earthward part of the plasma sheet is usually stable with respect to interchange motion, it has been long known that, under appropriate conditions, interchange-like instabilities are possible even in the ideal MHD approximations. Kadomtsev (1963) showed that the instability is developed if the plasma pressure has a steeper profile than L^{-7}. Safargaleev and Maltsev (1986) noted that interchange-like disturbances can arise even if there is no sharp boundary between areas with different plasma content. Taking into account that the considered optical phenomena were observed inside the auroral oval and that two other mentioned mechanisms (Lyatsky and Maltsev, 1984 and Jorgensen et al., 1999) imply the presence of a plasma boundary in the magnetosphere, we think that the interchange instability is more likely the reason for generation of omega auroras.

In accordance with Lui and Hamilton (1992), the radial profile of the quiet-time plasma pressure in the magnetotail exhibits a peak at L=3–4 and then decreases monotonically from L=4 and L=9. During magnetic storms, the advantageous pressure gradient is emphasized by the strong main-phase ring current injection (Sazykin et al., 2002). We think that the plasma injection accompanying the substorm onset also leads to a similar result.

In the dayside magnetospheric plasma, the necessary pressure gradient driving the interchange instability may take place, for example: i) during the periodic magnetopause oscillation that could lead to the formation of the gap between the central plasma sheet and the low-latitude boundary layer, as is frequently seen in the DMSP data (Newell and Meng, 1992, 1994); ii) during the periods of northward IMF B_z, when the magnetosheath plasma penetrates into the dayside magnetosphere via the reconnection process (Song and Russell, 1992). These possibilities were previously discussed by Lyatsky and Sibeck (1997) and Kozlovsky et al. (2003) in connection with the problem of the generation of different kinds of dayside auroras. Our data presented in Fig. 8 show that both the above-mentioned reasons for the development of an adequate plasma pressure gradient, somewhere inside the plasma sheet, could exist in our case. Indeed, the IMF B_z experienced the appreciable positive variations through the interval of interest. On the one hand, this might lead to the magnitopause oscillation and penetration of the magnetosheath plasma to the dayside magnetosphere. On the other hand, one can regard the trains of Ps6 in Fig. 8 as occurring (with certain delay) in response to the IMF B_z positive variations, since their appearance seems to be connected (both in time and in space) to the poleward displacement of the equatorial boundary of the electrojet following the northward turning B_z.

In the present case, we suggest that the substorm activity created favorable conditions for an instability development through the earthward injection of hot plasma. Then, these conditions were emphasized by IMF B_z positive variations, which finally led to a "triggering" of the Ps6/omega bands. We believe that the two above-mentioned effects could not produce Ps6/omega bands when acting separately. In the next section we will suggest a mechanism for torch formation also based on the interchange instability.

4.3 Possible scenario for torch formation

For 1 h after the substorm onset the electrojet expanded poleward, and the maximum of the pulsations also shifted to the north, moving from SOR to BJN. Then, near 06:00 UT the omega bands became visible to the TV camera running in Barentsburg, as some aurora undulations on the southern edge of the camera's field of view (see Fig. 6a). At approximately 06:03 UT, one of the bright tongues expanded poleward and evolved into a torch structure. For the next 7 min, the torch moved eastward and crossed the beam of the EISCAT radar in Tromsø. This allowed for measurements of the convection velocity close to one of the torch borders (the western border), which was finally shaped up at that time. At lower latitudes (inside the torch pedestal) the plasma flowed poleward, whereas an opposite flow was detected at higher latitudes (outside the torch), see Figs. 9 and 10. Such convection features partake of the interchange instability when the plasma tubes with higher β (the ratio of plasma pressure to magnetic pressure) move outward from the Earth and are replaced by plasma tubes with lower β, moving in opposite directions, respectively. The question is why do the relatively stable auroral forms – Ω-bands – become unstable?

It is well known that the highly conductive ionosphere suppresses the development of the interchange instability through the "frozen-in" conditions for the magnetic field lines (Swift, 1967). However, the field-aligned potential difference, $\phi_{||}$, can decouple the magnetosphere from the

ionosphere (Atkinson, 2001), and this, in principle, would allow for the instability to rise. The numerical simulations of omega bands carried out by Janhunen and Huuskonen (1993) supported this idea by showing a faster instability development when the field-aligned potential drop was included in the model. In our case the brightening of the small arc just before the torch formation indicated an increase in the arc-associated field-aligned current. Under appropriate conditions the increase of the current can result in the development of an anomalous resistivity region and field-aligned potential drop. The latter is supported by optical observations showing the decrease of the altitude of the brightening arc. So, just before the torch formation the magnetosphere became decoupled from the ionosphere in a limited area. That area is thought to also include the associated downward field-aligned current, the ionospheric signature of which – a dark hole in the background luminosity – we observed exactly in the place where the torch appeared a few minutes later (see Fig. 7). Recently, Aikio et al. (2004) presented a case study on the accelerated upward electrons above the "black auroras" observed by CLUSTER in response to auroral arc brightening (pseudobreakup event). They assumed that $\phi_{||}$ developed there as a result of an ionospheric feedback. In addition, the small ionospheric conductance in the dark area should also improve the conditions for the development of an instability.

Note that the local enhancement of discrete auroras poleward of the observation point was mentioned by Oguti et al. (1981) and Tagirov (1993) as characteristic pre-torch phenomena. We also observed a similar auroral feature before the second torch appearance at 06:14:35 UT. However, the second torch started deep inside the auroral oval, as one can conclude from the presence of discrete auroras northward of the torch (bottom series of images in Fig. 5). Such a situation occurred because of the displacement of the auroral oval poleward boundary, which was manifested as a gradual expansion of the auroral electrojet (Fig. 8, bottom panel) toward the north. Probably the location of the pre-existing arc further from the polar cap border hindered the instability development and the torch was not as impressive.

4.4 Brief comments concerning the similarity of the torch and breakup auroras

In fact, there is some similarity between auroral torches and substorm-related large-scale auroras – auroral bulge/surge. Both the torch and bulge are the result of a fast expansion of pre-existing auroras poleward. The shape of the auroral torch resembles the shape of the auroral bulge, but the azimuthal size of the former is smaller. By comparing the IMF conditions for substorms and omega auroras, Steen et al. (1988) supposed that both occurred during periods of enhanced convection and that the Kelvin-Helmholtz instability could be the origin of both phenomena. Later, to explain torch development, Tagirov (1993) applied the mechanism suggested by Lyatsky and Maltsev (1978) for bulge formation. Recently, Jorgensen et al. (1999) mentioned that "the presumed location of the magnetospheric source of Ω-bands has undergone a similar earthward motion as the presumed location of substorm onsets". We can extend the analogy of the torch with substorm activity by noting the following: 1) both are preceded by a short-lived brightening of discrete auroras: azimuthally-extended auroral arcs in the case of substorm onset (the so-called pseudo-breakup event) and azimuthally-restricted arc-like forms in the case of torch formation; 2) we connected the torch formation with the interchange instability arising due to the magnetosphere-ionosphere decoupling. Some investigators suggest this kind of instability as an explanation of the substorm onset, also pointing out the particular role of the field-aligned potential drop in its development (Stepanova et al., 2004).

5 Conclusions

We have presented here the results of multi-instrument observations of an auroral torch and Ps6 magnetic pulsations. Data from TV and ASC cameras in Barentsburg and Ny Ålesund, from EISCAT radars in Longyearbyen and Tromsø, as well as from the IMAGE network, have been used in this study. The auroral phenomenon we have considered differed from those discussed previously, as it occurred in an unusual place (high latitudes) and at an unusual time (late morning hours). The torch developed from one of the bright tongues of the omega bands, the presence and presumed location of which was inferred mainly from the Ps6 magnetic pulsations (series of positive spikes in the geomagnetic Y-component), since the cloudy conditions above northern Scandinavia hindered optical observations southward of Spitsbergen.

The following are the main results of our investigation:

1. Under suitable conditions in the interplanetary medium, magnetosphere deformation makes it possible to observe early-morning auroral zone phenomena (such as omega bands and auroral torches) at high latitudes and close to the noon.

2. In such a case, the IMF might be one more factor that influences the regime of the Ps6/omega bands. The above-discussed case study confirms this assumption, showing that only when acting together do substorm onset in the night sector and IMF B_z variations give rise to Ps6/omega-band generation.

3. In the event discussed here, the presumable source of Ps6/omega bands did not co-locate with convection reversal boundaries. This prevents us from interpreting the phenomena in the framework of the Kelvin-Helmholtz instability. We assume that the interchange instability is responsible for both the omega bands and the auroral torch generation. This kind of instability is also discussed in the literature in connection with omega auroras.

4. Some numerical characteristics of the auroral torch were obtained. The torch propagation was eastward at

a velocity of ∼600 m/s, very close to the direction and the velocity of the background ionospheric convection (measured 400 km west of the observational point). Inside the torch plasma moved poleward at a velocity of 100–200 m/s (the latter value refers to torch bright border), whereas outside the west border of the torch the plasma flowed in the opposite direction at a velocity of ∼300 m/s. Since we were able to measure only the line-of-sight component, the velocities mentioned are the (geomagnetic) azimuthal and meridional components of convection velocity. The height of the most poleward point of the torch was slightly higher than previously reported for early morning torches, but lower than that typical for the dayside auroras.

5. We emphasized the dark hole in the background luminosity and short-lived azimuthally-restricted auroral arcs as possible precursors of the auroral torch. We think that these auroral features should be further studied because they can provide useful insights into the mechanism of auroral torch generation.

Acknowledgements. We thank for cooperation of Kakioka (JMA), Honolulu and San Juan (USGS), Hermanus (RSA), Alibag (IIG) and CRL, INTERMAGNET and many others to make QL-D_{st} in near real time. We acknowledge the geomagnetic observatories CBB, IQA, GH (Geological Survey of Canada), GDH (Danish Meteorological Institute), JAN (Tromsø Geophysical Observatory) for magnetic data. The solar wind and IMF data from the WIND satellite were obtained from the CDAWeb ISTP Key Parameter database (data providers are K. Olgivie and R. Lepping at NASA). Work on OVATION has been conducted by scientists at The Johns Hopkins University Applied Physics Laboratory, at the University of Alaska, Fairbanks, and at the Air Force Research Laboratory. We thank B. Holmeslet (University of Tromsø), O. Rasmussen (Danish Meteorological Institute), W. Glegolski (Institute of Geophysics of Polish Academy of Sciences) and J. Posch (Augsburg College) for supplying us near-real time magnetic data, as well as K. Kauristie (FMI) for providing LYR and KIL ASC images for selected intervals. We are indebted to the Director and staff of EISCAT for operating the facility and supplying the data. EISCAT is an International Association supported by Finland (SA), France (CNRS), the Federal Republic of Germany (MPG), Japan (NIPR), Norway (NFR), Sweden (NFR) and the United Kingdom (PPARC). We thank R. Kuula at Space Research Group of the Oulu University for the EISCAT data analysis. The work of V. Safargaleev was supported by Svenska Institutet (VISBY Programme stipend). The work of A. Kozlovsky was funded by the Academy of Finland. The work of A. Kotikov was supported by Kungliga Vetenskapsakademin.

Topical Editor T. Pulkkinen thanks T. S. Trondsen and another referee for their help in evaluating this paper.

References

Aikio, A., Mursula, K., Buchert, S., Forme, F., Amm, O., Marklund, G., Dunlop, M., Fontain, D., Vaivadas, A., and Fazakerly, A.: Temporal evolution of auroral arcs as measured by the CLUSTER satellites and coordinated ground-based instruments, Ann. Geophys., 22, 4089-4101, 2004,
SRef-ID: 1432-0576/ag/2004-22-4089.

Akasofu, S.-I. and Kimball, D. S.: The dynamics of aurora, 1, Instabilities of aurora, J. Atmos. Terr. Phys., 28, 205–211, 1964.

Akasofu, S.-I.: A study of auroral displays photographed from DMSP-2 satellite and from the Alaska meridian chain of stations, Space Sci. Rev., 16, 617–725, 1974.

Amm, O.: Improved electrodynamic modeling of an omega band and analysis of its current system J. Geophys. Res., 101, no. A2, 2677-2684, 1996.

André, D. and Baumjohann, W.: Joint two-dimensional observations of ground magnetic and ionospheric electric fields associated with auroral currents. 5. Current system associated with eastward drifting omega bands, J. Geophysics, 50, 194–201, 1982.

Atkinson, G.: Decoupling of convection in the magnetosphere from the ionosphere by parallel electric fields, AGU Fall Meeting 2001, abstract No SM51A-0784, AGU, 2001.

Connors, M. and Rostoker, G.: Source mechanisms for morning auroral features, Geophys. Res. Lett., 20, 1535–1538, 1993.

Connors, M., Rostoker, G., Sofko, G., McPherron, R. L., Henderson, M. G.: Ps6 disturbances: relation to substorms and the auroral oval, Ann. Geophys., 21, 493–508, 2003,
SRef-ID: 1432-0576/ag/2003-21-493.

Elphinstone, R. D., Hearn, D. J., Murphree, J. S., Cogger, L. L., Jonson, M. L., and Vo, H. B.: Some UV dayside auroral morphologies, in: Auroral Plasma Dynamics, Geophys. Monogr., 80, AGU, Washington, D.C., 13–45, 1993.

Guzdar, P. N., Shao, X., Goodrich, C. C., Papadopoulos, K., Wiltberger, M. J.,and Lyon, J. S.: Three-dimensional MHD simulations of the steady state magnetosphere with northward interplanetary magnetic field, J. Geophys. Res., 106, 257–288, 2001.

Janhunen, P. and Huuskonen, A.: A numerical ionosphere-magnetosphere coupling model with variable conductivities, J. Geophys. Res., 98, 9515–9530, 1993.

Jorgensen, A. M., Spence, H. E., Huges, T. J., and McDiarmid, D.: A study of omega bands and Ps6 pulsations on the ground, at low altitude and at geostationary orbit, J. Geophys. Res., 104, 14 705–14 715, 1999.

Kadomtsev, B. B.: Stability of plasma. In: Problems of the theory of plasma, edited by: Leonovich, M. A., 2, 132–176, 1963.

Kawasaki, K. and Rostoker, G.: Perturbation magnetic fields and current systems associated with eastward drifting auroral structures, J. Geophys. Res., 84, 1464–1480, 1979.

Kotikov, A. L., Bolotenskaia, B. D., Gizler, V. A., Troshichev, O. A., and Pashin, A. B.: Structure of auroral zone phenomena from the data of meridional chains of stations: magnetic disturbances in the nighttime auroral zone and auroras, J. Atmos. Terr. Phys., 51, 265–274, 1991.

Kozlovsky A., Safargaleev, V., Jussila, J., and Koustov, A.: Prenoon high-latitude auroral arcs as a manifestation of the interchange instability, Ann. Geophys., 21, 2303–2314, 2003.

Lyatsky, W. B. and Maltsev, Yu. P.: Origin of the auroral bulge (Engl. transl.), Geomagn. Aeron., 24, 71–75, 1984.

Lyatsky, W. and Sibeck, D.: Central plasma sheet disruption and the formation of dayside poleward moving auroral events, J. Geophys. Res., 102, 17 625–17 630, 1997.

Lui, A. T. Y. and Hamilton, D. C.: Radial profiles of quit time magnetospheric parameters, J. Geophys. Res., 97, 19 325–19 332, 1992.

Lühr, H. and Schlegel, K.: Combined measurements of EISCAT and the EISCAT magnetometer cross to study Ω-bands, J. Geophys. Res., 99, 8951–8959, 1994.

Maltsev, Yu. P. and Rezhenov, B. V.: Statistical study of the re-

sponse of Dst index to the change of the solar wind dynamic pressure (Engl. transl.), Geomagn. Aeron., 42, 175–178, 2002.

Meng, C.-I.: Dynamic variation of the auroral oval during intense magnetic storm, J. Geophys. Res., 89, 227–235, 1984.

Newell, P. T. and Meng, C.-I.: Mapping the dayside ionosphere to the magnetosphere according to particle precipitation characteristics, Geophys. Res. Lett., 19, 609–612, 1992.

Newell, P. T. and Meng, C.-I.: Ionospheric projections of magnetospheric regions under low and high solar wind pressure conditions, J. Geophys. Res., 99, 273–286, 1994.

Oguti, T., Kokubun, S., Hayashi, K., Tsuruda, K., Machida, S., Kitamura, T., Saka, O., Watanabe, T.: An auroral torch structure as an active center of pulsating auroras, Can. J. Phys., 59, 1056–1062, 1981.

Opgenoorth, H. J., Oksman, J., Kaila, K. U., Nielsen, E., and Baumjohann, W.: Characteristic of eastward drifting omega bands in the morning sector, J. Geophys. Res., 88, 9171–9185, 1983.

Opgenoorth, H. J., Persson, M. A. L., Pulkinen, T. J., and Pellinen, R. J.: Recovery phase of magnetospheric substorms and its association with morning sector aurora, J. Geophys. Res., 99, 4115–4129, 1994.

Pulkkinen, T. I., Pellinen, R. J., Koskinen, H. E. J., Opgenoorth, H. J., Murphree, J. S., Petrov, V., Zaitsev, A., and Friis-Christensen, E.: Auroral signatures of substorm recovery phase: A case study, in: Magnetospheric Substorms, edited by: Kan, J. R., Potemra, T. A., Kokubun, S., and Iijima, T., Geophys. Monogr. Ser., vol. 64, AGU, Washington, D.C., 333–342, 1991.

Rostoker, G. and Samson, J. S.: Can substorm expansive phase effects and low frequency Pc magnetic pulsations be attributed to the same source mechanism? Geophys. Res. Lett., 11, 271–274, 1984.

Saito, T.: Long-period irregular micropulsations, Pi3, Space Sci. Rev., 21, 427–467, 1978.

Safargaleev, V. V. and Maltsev, Yu. P.: Internal “gravity” waves in the plasma sheet (Engl. transl.), Geomagn. Aeronomy, 26, 220–224, 1986.

Safargaleev, V. V., Kozlovsky, A. E., Osipenko, S. V., and Tagirov, V. R.: Azimuthal expansion of high latitude auroral arcs, Ann. Geophys., 21, 1793–1805, 2003,
SRef-ID: 1432-0576/ag/2003-21-1793.

Sazykin, S., Wolf, R. A., Spiro, R. W., Gombosi, T. I., De Zeeuw, D. L., and Thomsen, M. E.: Interchange instability in the inner magnetosphere associated with geosynchronous particle flux decreases, Geophys. Res. Lett., 29, 81–1, doi:10.1029/2001GL014416, 2002.

Shiokawa, K. T., Ogino, T., Hayashi, K., and McEven, D. J.: Quasi-periodic poleward motion of morningside sun-aligned arcs: A multievent study, J. Geophys. Res., 102, 24 325–24 332, 1997.

Solovyev, S. I., Baishev, D. G., Barkova, E. S., Engebretson, M. J., Posh, J. L., Huges, W. J., Yumoto, K., and Pilipenko, V. A.: Structure of disturbances in the dayside and nighside ionosphere during periods of negative interplanetary magnetic field Bz, J. Geophys. Res., 104, 28 019–28 039, 1999.

Song, P. and Russell, C. T.: Model of the formation of the low-latitude boundary layer for strongly northward interplanetary magnetic field, J. Geophys. Res., 97, 1411–1420, 1992.

Steen, A., Collis, P. N., Evans, D., Kremser, G., Capelle, S., Rees, D., and Tsurutani, B. T.: Observation of a gradual transition between Ps6 activity within auroral torches and surgelike pulsations during strong geomagnetic disturbances, J. Geophys. Res., 93, 8713–8733, 1988.

Stepanova, M. V., Antonova, E. E., Bosqued, J. M., and Kovrazhkin, R.: Radial plasma pressure gradients in the high latitude magnetosphere as sources of instabilities leading to the substorm onset, Adv. Space Res., 33, 761–768, 2004.

Swift, D. W.: The possible relationship between the auroral breakup and the interchange instability of the ring current, Planet. Space Sci., 15, 1225–1238, 1967.

Tagirov, V.: Auroral torches: results of optical observations, J. Atmos. Terr. Phys., 55, 1775–1787, 1993.

Trondsen, T. S., Lyatsky, W., Cogger, L. L., and Murphree, J. S.: Interplanetary magnetic field control of dayside auroras, J. Atmos. Terr. Phys., 61, 829–840, 1999.

Wild, J. A., Yeoman, T. K., Eglitis, P., and Opgenoorth, H. J.: Multi-instrument observations of the electric and magnetic field structure of omega bands, Ann. Geophys., 18, 99–110, 2000,
SRef-ID: 1432-0576/ag/2000-18-99.

Yamamoto, T., Inoe, S., and Meng, C.-I.: Formation of auroral omega bands in the paired region 1 and region 2 field-aligned current system, J. Geophys. Res., 102, 2531–2544, 1997.